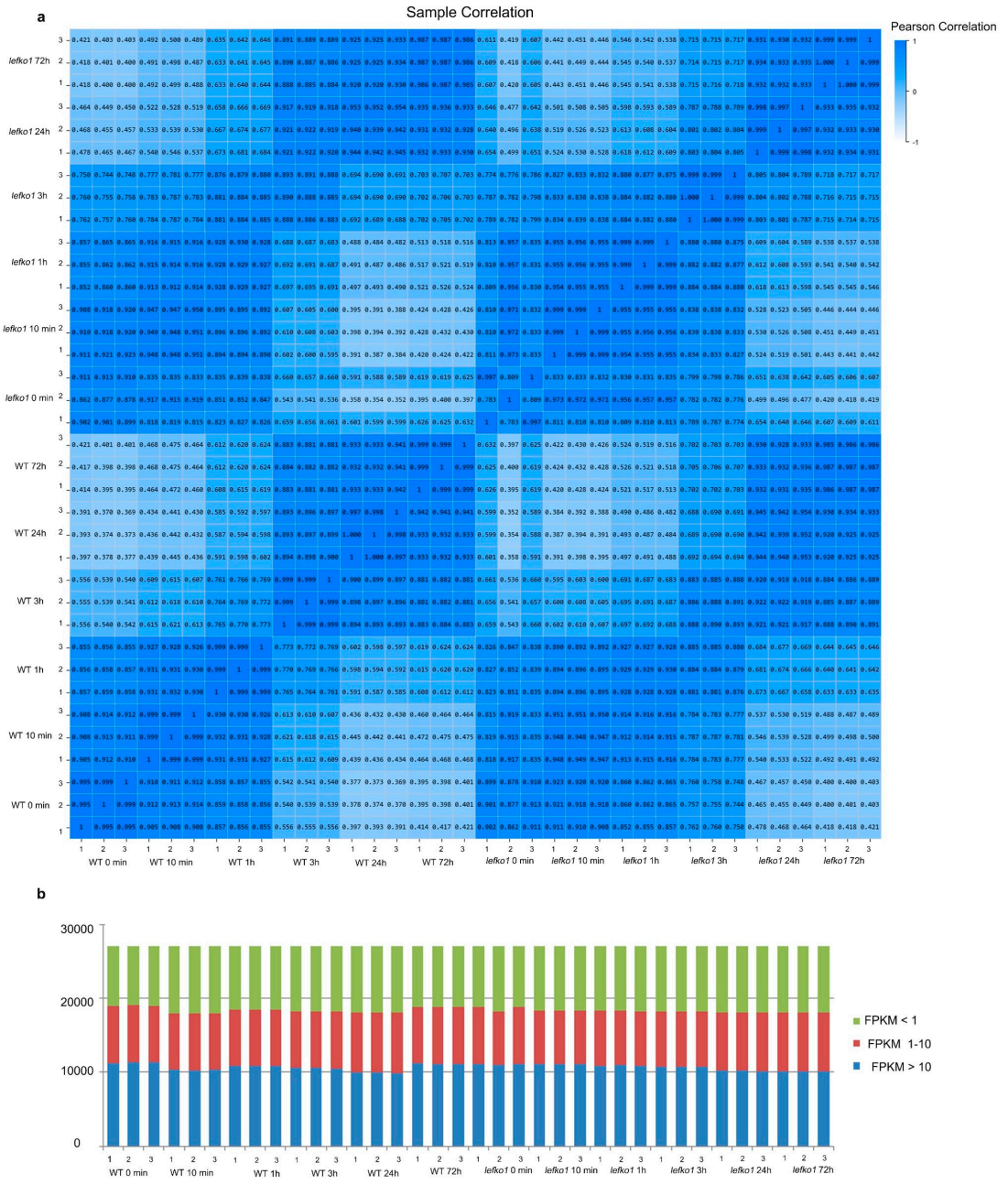
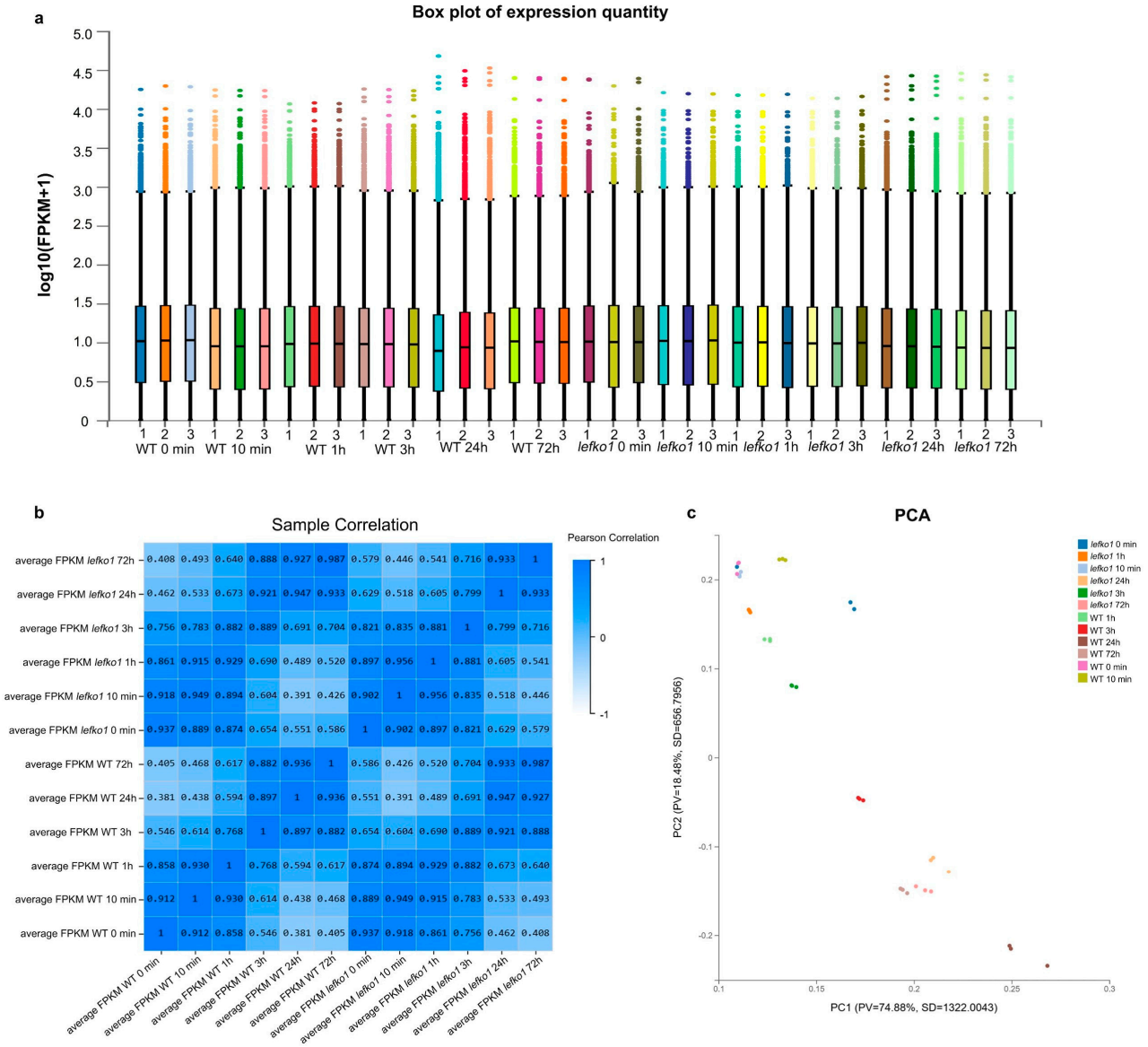


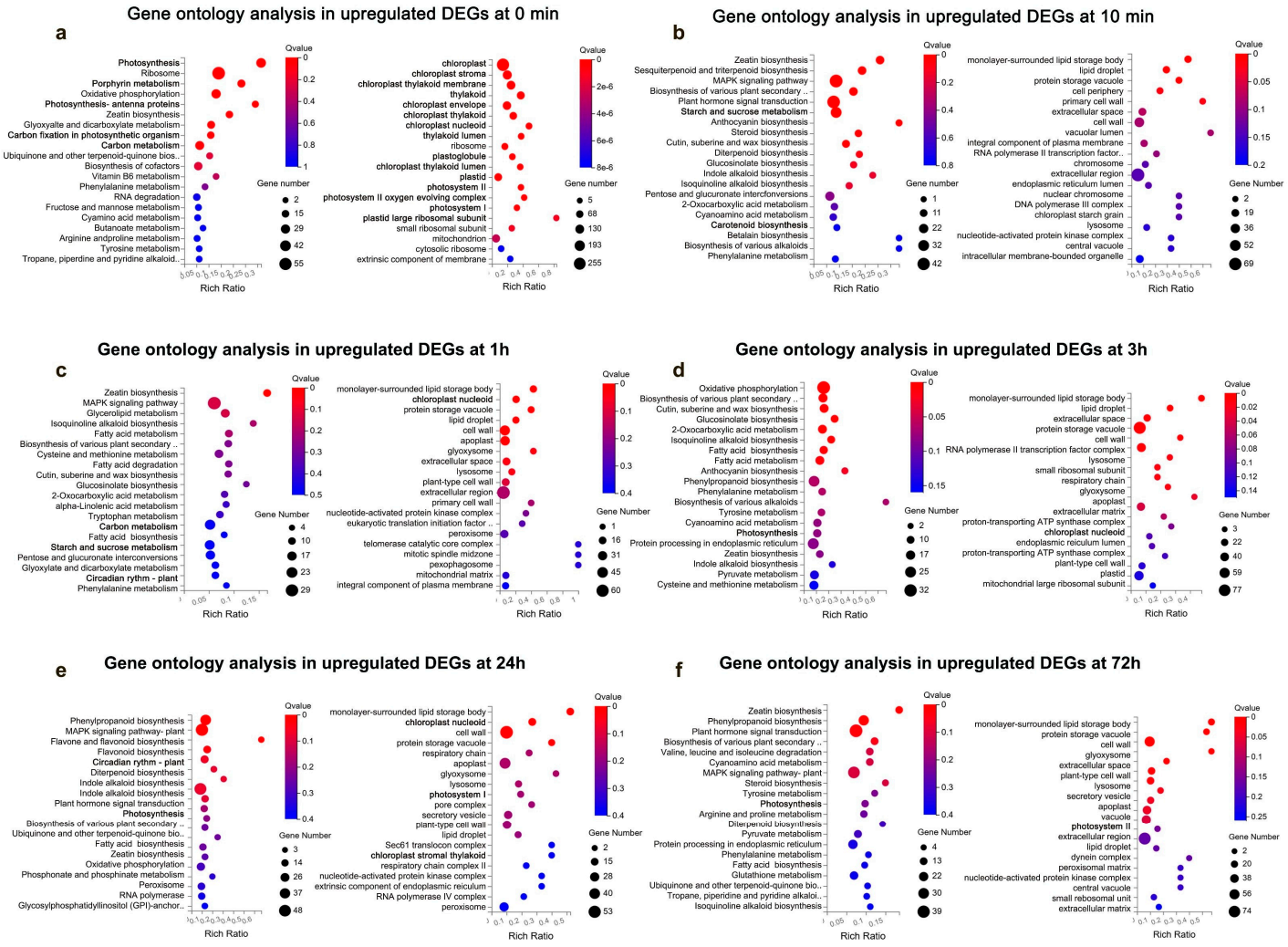
Supplementary Figure S1. Quality evaluation of RNAseq data.

a) Pearson Correlation of RNAseq samples to evaluate the global similarity or reproducibility between samples. b) FPKM (Fragments Per Kilobase of exon per Million fragments mapped) normalized measurements to estimate gene or transcript abundance from RNA-seq data. By normalizing for both sequencing depth (per million fragments) and gene length (per kilobase), FPKM allows for accurate comparisons of expression levels—either between different genes within the same sample or for the same gene across different samples.



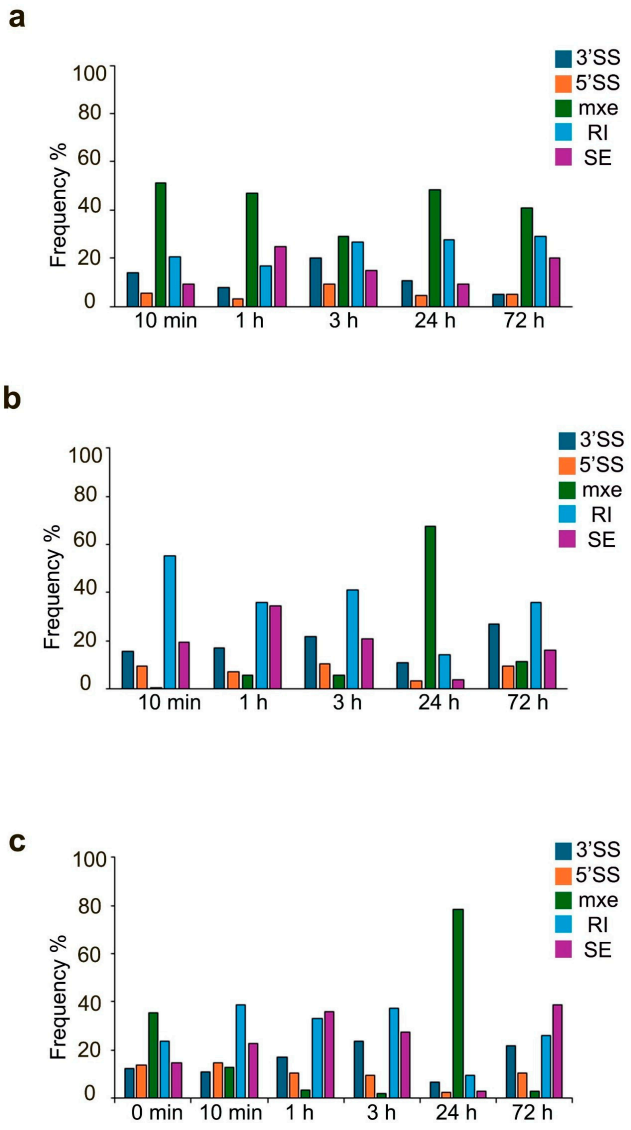
Supplementary Figure S2. Assessment of RNAseq sample similarity, normalization effectiveness, identification of potential outliers, and assessment of sample clustering and quality.

a) A box plot of expression quantity of the indicated RNA-seq samples to display the distribution of gene expression levels by FPKM across the multiple samples. b) Pearson correlation of the groups of RNAseq samples. c) PCA (Principal Component Analysis) of RNA-seq samples to visualize relationships, detect outliers, and identify the main sources of variation across high-dimensional gene expression samples.

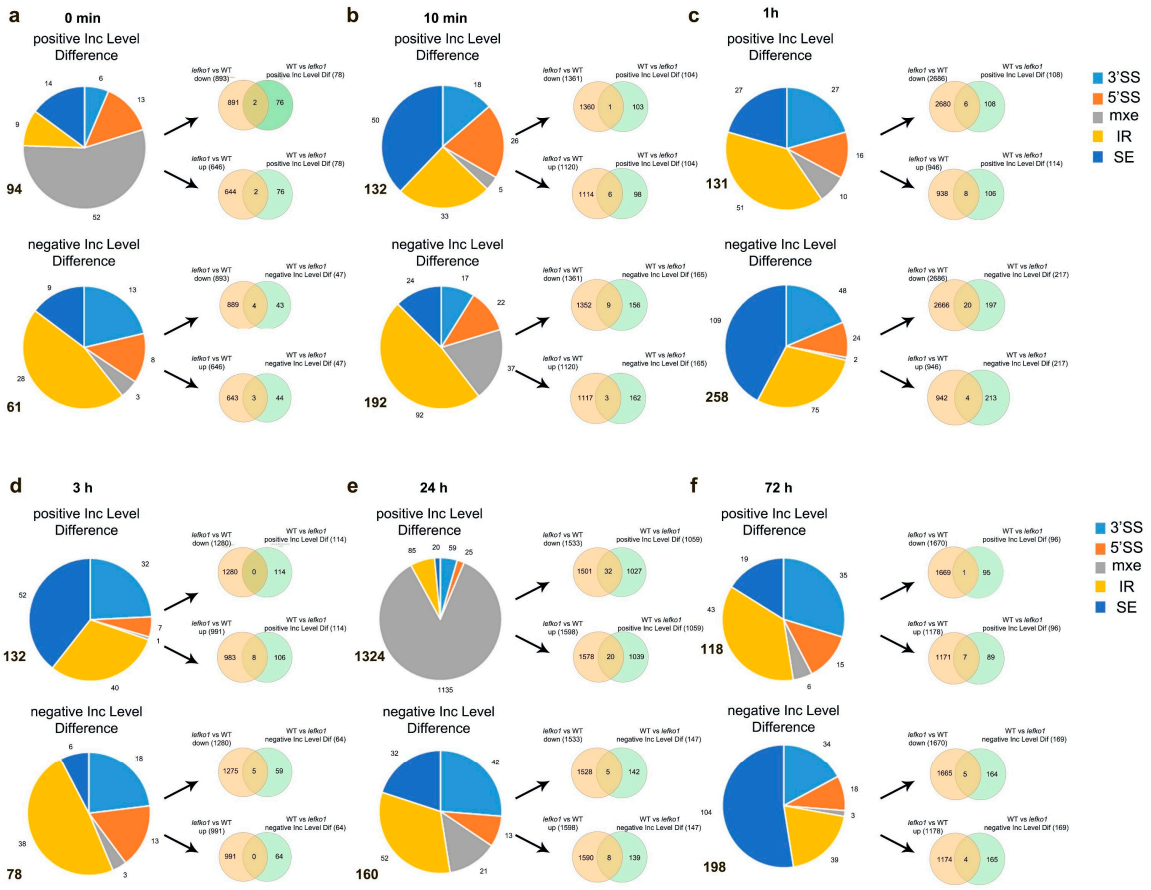


Supplementary Figure S3. Gene ontology enrichment analysis of the upregulated DEGs in the time series transcriptomic analysis of wild-type and *lefko 1* seedlings upon light exposure.

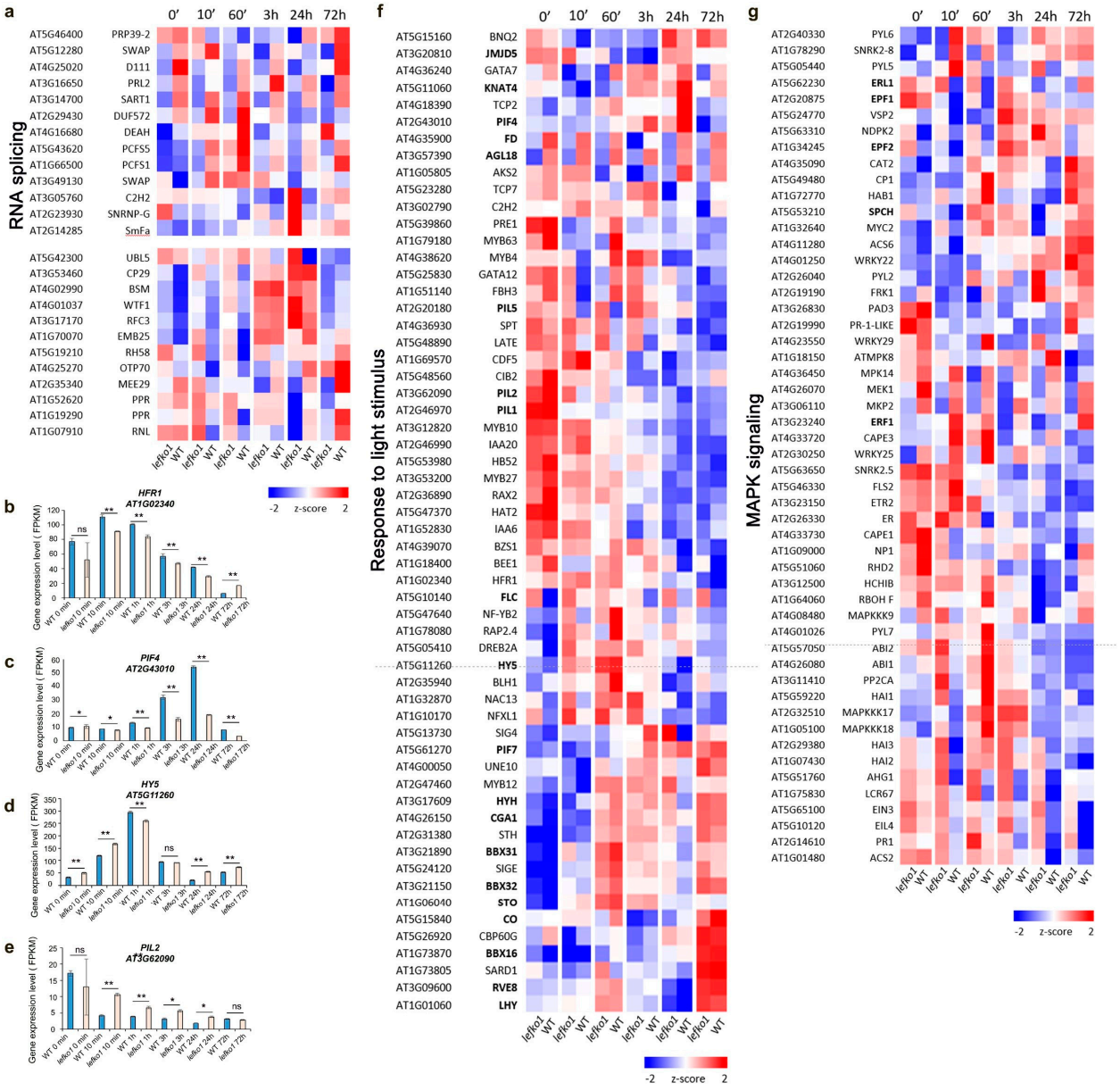
a-f) Bubble charts of the top 20 KEGG pathways and Cellular Compartment enrichment analysis of upregulated DEGs for time 0 min (c), time point 10 min (d), time point 1h (e), time point 3h (f), time point 24h (g), and time point 72h (h).



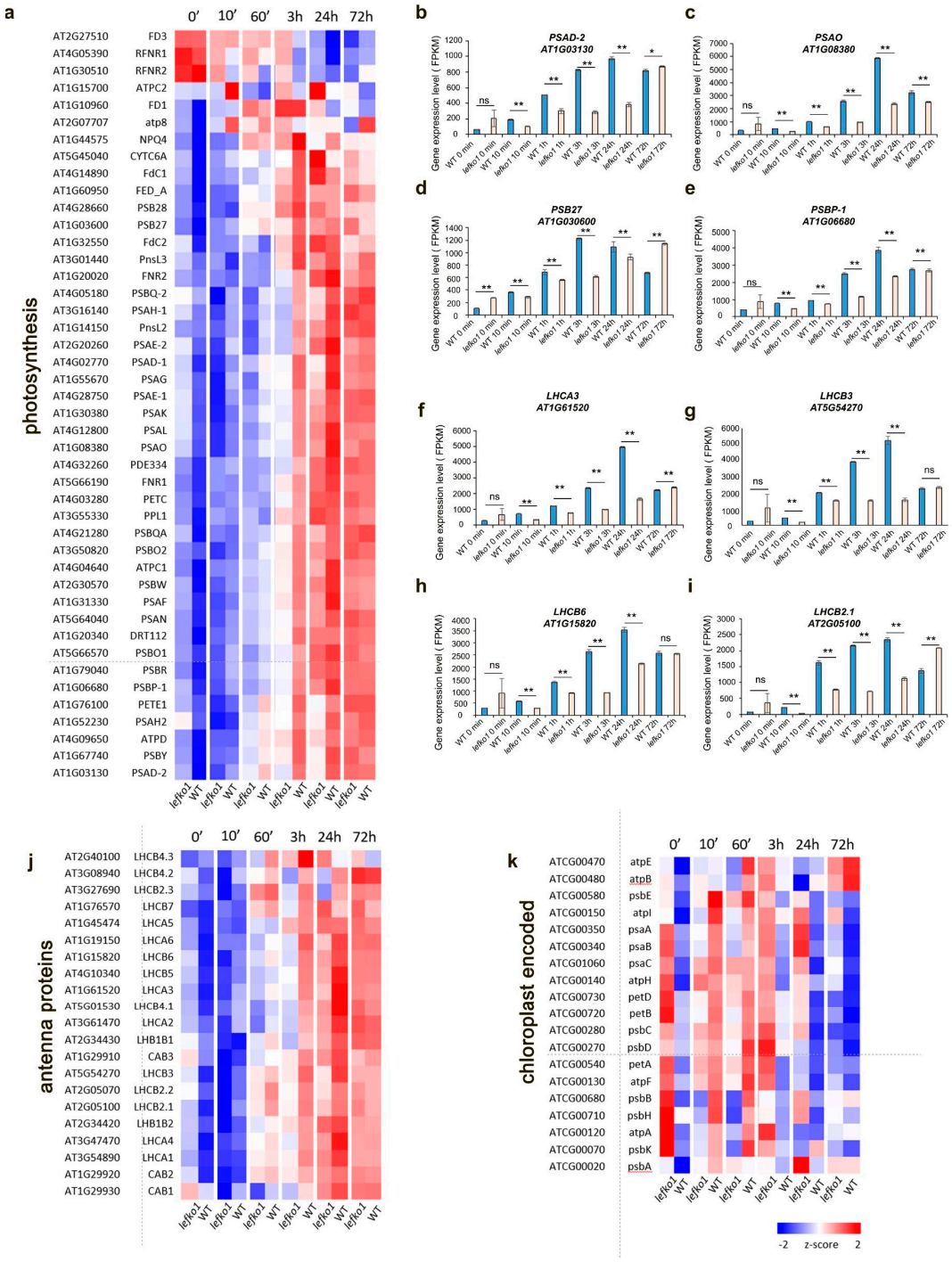
Supplementary Figure S4. Analysis of the frequencies of the Alternative Splicing events in wild-type and *lefko 1* seedlings during light response. a, b) Diagrams showing the frequencies of each type of Alternative Splicing during the time series exposure to light in wild-type (a) or *lefko 1* (b) seedlings. The five modes of alternative splicing events, including 3SS, 5SS, mxe, IR, and SE, are shown. Each time point is compared to time point 0 min (etiolated seedlings). c) Diagram showing the frequency of defects for each type of alternative splicing deriving from the pairwise comparison of wild type versus *lefko 1* seedlings at the indicated time points upon light exposure. FDR< 0.05.



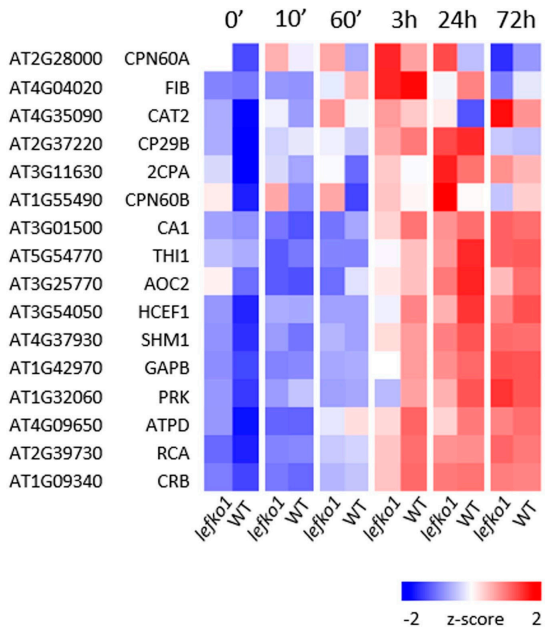
Supplementary Figure S5. Splicing events in genes are distinct from DEGs in *lefko 1* seedlings during early light response. a-f) Pie charts illustrating the number of alternative splicing defects with positive or negative Inclusion Level Difference in the pairwise comparison of wild-type versus *lefko 1* seedlings at the indicated time points of light response (FDR< 0.05). The five modes of alternative splicing events, including 3SS, 5SS, mxe, IR, and SE, are shown. Venn diagrams in yellow showing the number of down- or upregulated genes (|log2FC|>1) in the pairwise comparison of *lefko 1* versus wild-type, venn diagrams in green showing the splicing defects with Inc Level Dif> or <0, and Venn diagrams in orange showing the intersections in each case.



Supplementary Figure S6. Impaired function of LEFKOTHEA affects the expression of genes involved in RNA splicing, MAPK signaling, and light response pathways. a, f, g) Heatmaps depicting the clustering of the differentially expressed genes belonging to the "RNA splicing" (a), transcription factors belonging to "Response to light stimulus" (f), and differentially expressed genes belonging to "MAPK signaling" terms identified in all *lefko 1* to wild type comparisons (g). Each row depicts the z-score of the log2-transformed FPKM of each gene, whereas each column represents the time point. Only genes with FPKM>1 in most of the timepoints were included in the analysis. Variations in gene expression level are shown by a gradient color scale (red: higher expression; blue: lower expression). b-e) Transcript levels of the indicated light-related genes. Data are presented as mean ± SD of three biological repetition for each sample; error bars represent SDs. Data were analyzed by t-test. *, $P < 0.05$; **, $P < 0.01$; ns, non-significant.



Supplementary Figure S7. LEFKOTHEA affects the expression of genes involved in photosynthesis and the structure of the photosynthetic apparatus during the response to light. a, j, k) Heatmap depicting the clustering of the genes belonging to "Photosynthesis" (a) and "Antenna proteins"(j) terms, as well as the chloroplast-encoded genes (k) identified in all *lefko 1* to wild type comparisons. Each row depicts the z- score of the log2-transformed FPKM of each gene, whereas each column represents the time point. Only genes with FPKM>1 in most of the timepoints were included in the analysis. Variations in gene expression level are shown by a gradient color scale (red: higher expression; blue: lower expression). b-i) Transcript levels of the indicated genes. Data are presented as mean ± SD of three biological repetition for each sample; error bars represent SDs. Data were analyzed by t-test. *, $P < 0.05$; **, $P < 0.01$; ns, non- significant.



Supplementary Figure S8. LEFKOTHEA regulates the expression of genes encoding proteins that localize at stromules during the response to light. Heatmap depicting the clustering of the DEGs belonging to the "Stromules" term identified in all *lefko 1* to wild type comparisons. Each row depicts the z-score of the log2-transformed FPKM of each gene, whereas each column represents the time point. Only genes with FPKM>1 in most of the timepoints were included in the analysis. Variations in gene expression level are shown by a gradient color scale (red: higher expression; blue: lower expression).